AD-A187 582 THE MAGIC OF CARRIER PATTERNS IN MOIRE INTERFEROMETRY 1/1
(U) VIRGINIA POLYTECHNIC INST AND STATE UNIV BLACKSBURG
DEPT OF E.. Y GUO ET AL. AUG 87 N00014-86-K-0255
UNCLASSIFIED F/G 11/4 NL

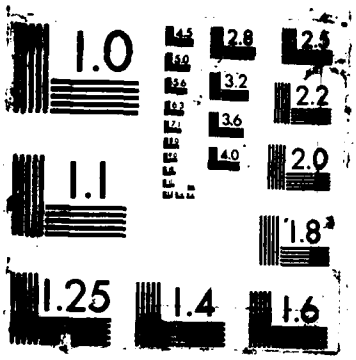
1.0
1.1
1.25
1.4
1.6
1.8
2.0
2.2
2.5
2.8
3.2
3.6
4.0

Contract N00014-86-K-0255

THE MAGIC OF CARRIER PATTERNS IN MOIRE INTERFEROMETRY

Y. Guo, D. Post, R. Czarnek

Virginia Polytechnic Institute and State University
Engineering Science and Mechanics Department
Blacksburg, Virginia 24061

SPIE Conf.
August '87

ABSTRACT

Practical applications in which carrier patterns are used with moire interferometry for strain measurements are presented. Examples of typical experimental analyses illustrate how moire carrier patterns are applied to obtain the desired data in complex laminated composite specimens. In many cases, carrier patterns permit extraction of much more detailed information, with procedures that are easier and more accurate than those using load-induced fringes alone. In moire interferometry, the carrier patterns can be introduced easily by adjustments of optical elements that control the virtual reference grating.

1.0 INTRODUCTION

The carrier pattern is an important ingredient in moire interferometry. Together with other special properties, it makes moire interferometry a unique and powerful technique for displacement and strain measurements. Carrier patterns can be used for various purposes, including the following:

1. to increase the accuracy of extracting data from a fringe pattern
2. to distinguish the signs of the displacements by introducing a carrier pattern of known sign
3. to determine fringe gradients where they are not adequately represented in the load-induced fringe patterns
4. to cancel the initial or no-load fringe pattern
5. to measure in-plane and out-of-plane displacements simultaneously

All the applications mentioned above have their own magic qualities. In this paper, point 3 is illustrated by several examples. The details of other applications can be found in references [1]-[5].

2.0 MOIRE INTERFEROMETRY

2.1 Basic Principle

The principle of moire interferometry is depicted in Fig. 1, together with the relevant equations [1]. In this method, a diffraction grating is replicated on the specimen and it deforms together with the loaded specimen. The virtual reference grating created by interference of two coherent beams B1 and B2 is superimposed on the specimen grating. The specimen and reference gratings form a fringe pattern which is a contour map of in-plane specimen displacements U and V. This pattern is photographed with a camera focused on the specimen surface. In Fig. 1, f is the frequency of the virtual reference grating, N is the fringe order at each point in the moire pattern and ε and γ are normal and shear strains, respectively. In this work, f = 2400 lines/mm.

2.2 Moire Carrier Patterns

The carrier pattern has also been called mismatch fringes in geometric moire [2,3]. It can be introduced by changing the direction or the frequency of the reference grating. In geometric moire, a real grating is used as a reference grating, so it has to be interchanged with another reference grating whenever its frequency needs to be changed. The change is much easier in moire interferometry. By adjusting the direction of the incident beam B1 or B2 (Fig. 1), the virtual reference grating in moire interferometry can be changed very easily both in direction and in frequency. Experimentally, this is usually done by a thumbscrew adjustment of one optical element, e.g., a mirror that directs light into B1. A carrier pattern of extension, comprised of fringes parallel to the lines of the reference grating, is obtained by a small change of the magnitude of angle 2α. A carrier pattern of rotation, comprised of fringes essentially perpendicular to the lines of the reference grating, is obtained by a small rotation of the plane of B1 and B2 about their

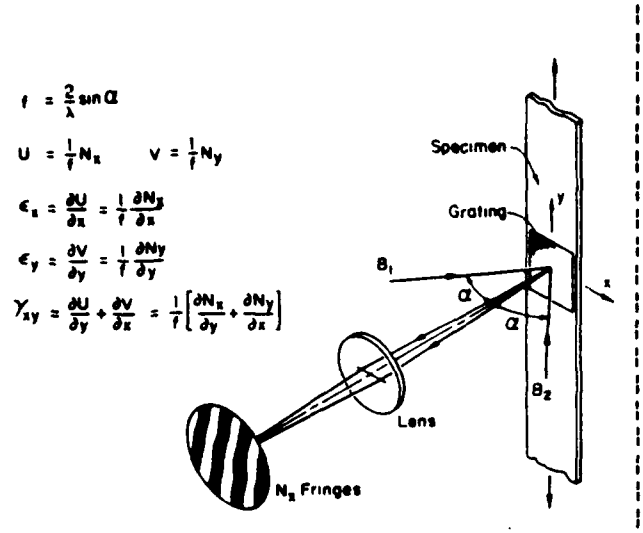

Fig. 1. Moire Interferometry and the Relevant Equations.

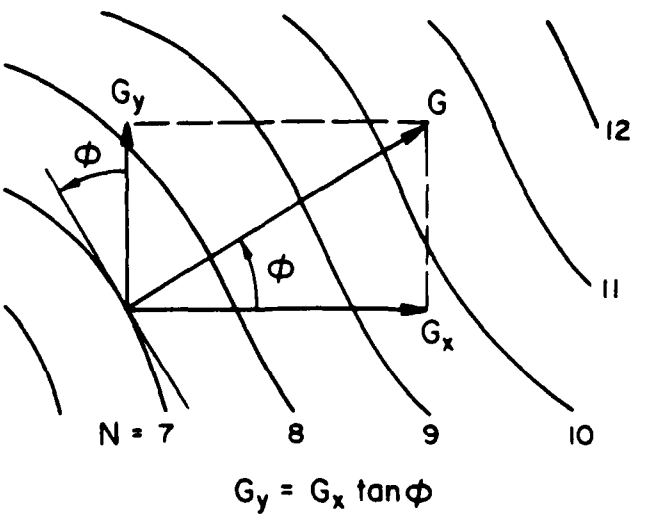

Fig. 2. Fringe Gradient and Fringe Slope.

bisector, or by a rotation of the specimen around its normal axis. The carrier pattern of extension produces an apparent uniform normal strain, tensile or compressive, on the specimen surface. The carrier pattern of rotation produces fringes equivalent to those of a rigid body rotation of the specimen.

2.3 Fringe Gradients and Strains

At an arbitrary point of a fringe pattern, the fringe gradient (fringes per mm) can be defined by two orthogonal components: the gradient in the x direction, G_x, and the gradient in the y direction, G_y. These two components are independent of each other and related by the equation

$$G_y = G_x \tan\phi \tag{1}$$

where $\tan\phi$ is the slope of the fringe at that point, as illustrated in Fig. 2.

By judicious use of carrier patterns, a fringe gradient in one direction can be modified without changing the gradient in the other direction. Moreover, if the fringe gradient in one direction is known, the gradient in the other direction can be determined from the slope ($\tan\phi$) of the fringes. These properties will be used to advantage in the following sections.

With knowledge of the fringe gradient and the components of the fringe gradient, the displacement derivatives can be calculated by the following equations and the strains can be calculated by the equations of Fig. 1.

For the U (x direction) displacement field

$$\frac{\partial U}{\partial x} = \frac{1}{f} G_x \quad ; \qquad \frac{\partial U}{\partial y} = \frac{1}{f} G_y \tag{2}$$

For the V (y direction) displacement field

$$\frac{\partial V}{\partial y} = \frac{1}{f} G_y \quad ; \qquad \frac{\partial V}{\partial x} = \frac{1}{f} G_x \tag{3}$$

3.0 APPLICATIONS OF CARRIER PATTERNS

3.1 Specimens

In the studies illustrated here, the specimens were all made of laminated fiber-reinforced composite materials. For experimental analyses of the behavior of these complex structural bodies, moire interferometry and its carrier patterns have provided an excellent and unique approach.

3.2 Carrier Fringes Parallel to the Initial Fringes

Figure 3 shows a rail-shear test for determination of interlaminar shear properties of a graphite/epoxy specimen. The cross derivative $\partial V/\partial x$ is very high and the fringes are nearly vertical, as shown in the V displacement pattern [Fig. 3b]. If the gradient $\partial V/\partial y$ is desired, its determination from this pattern would be difficult. By introducing carrier fringes of rotation, which are nearly parallel to the initial fringes, $\partial V/\partial x$ is minimized, but the gradient in the y direction remains unchanged. This is illustrated in Fig. 3c, from which the normal strain $\partial V/\partial y$ can be obtained easily and with high accuracy. Here, the carrier fringes cancel G_x fringes of the load-induced pattern.

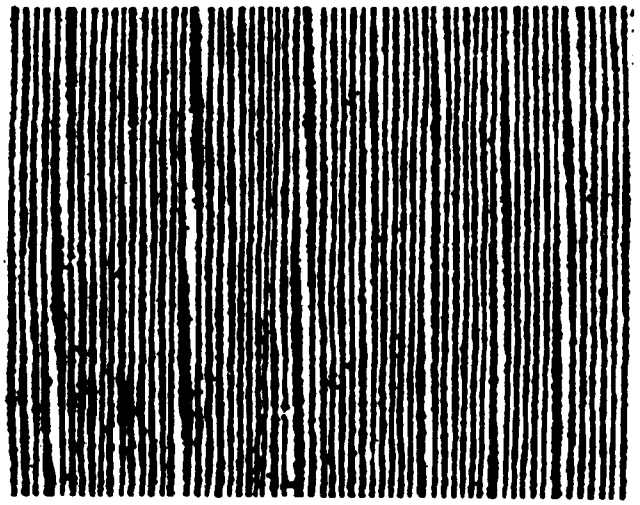

b. Load-induced fringe pattern of the V field for portion of specimen in dashed box

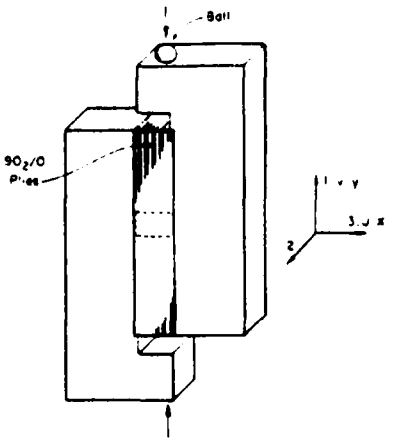

a. Specimen and loading fixture

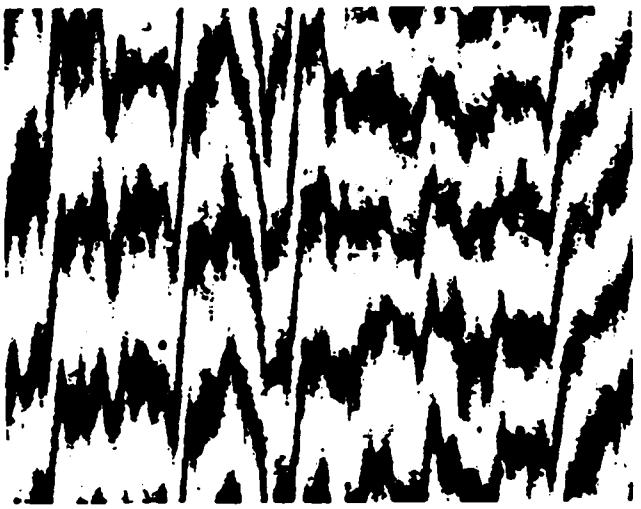

c. Load-induced fringes with carrier of rotation

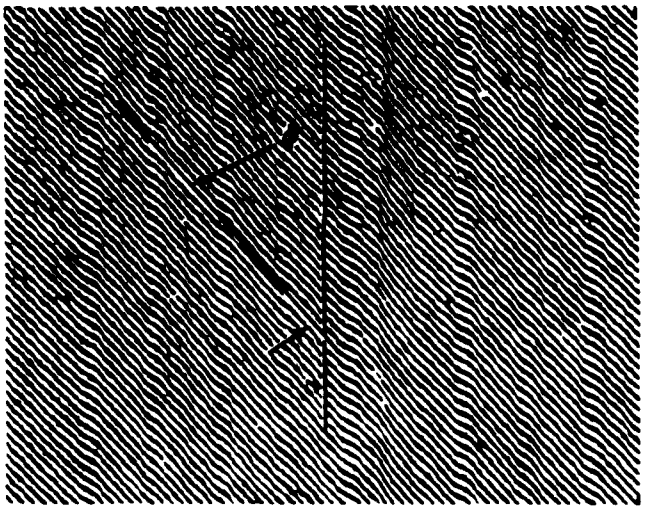

d. Load-induced fringes with carrier of extension

Fig. 3. Rail-shear Test for Interlaminar Shear Properties of [90/90/0]n Graphite/Epoxy Composite Specimen.

3.3 Carrier Fringes Perpendicular to the Initial Fringes

If the component of shear strain $\partial V/\partial x$ is required from Fig. 3b, the fringe gradient in the x direction has to be measured. In certain layers of this specimen, the deformations are represented by only one fringe. It is impossible to measure the gradient by only one fringe unless a sophisticated grey-level technique with very high spatial resolution is applied. By introducing a carrier pattern of extension, the fringe pattern is transformed to that in Fig. 3d. The fringe gradient in the x direction can be calculated as $G_x = G_y/\tan\phi$ [Eq. (1)]. Here, G_y is the gradient of introduced carrier fringes and $\tan\phi$ is the slope of the resulting fringe. G_y is a constant and it is easily determined from Fig. 3d, while the fringe slope is measured for each location. Since the carrier pattern in the y direction doesn't change the fringe gradient in the x direction, G_x still represents the required gradient $\partial V/\partial x$ in Fig. 3b. Although these gradients could not be recognized from Fig. 3b, the distribution of $\partial V/\partial x$ across the width of the specimen can be extracted from Fig. 3d with high fidelity.

Figure 4 is an example of using a perpendicular carrier pattern to deal with the nonuniformity problem. The specimen is a 48 ply quasi-isotropic beam of graphite-PEEK in a five-point bending test [6]. Fig. 4b depicts the load-induced U displacement field. The pattern is complicated and it is difficult to assign fringe orders with certainty. In addition, there are insufficient fringes in the central region to determine the strain in each ply. However, carrier fringes of extension transform the pattern to that of Fig. 4c. Now, the fringes can be traced without ambiguity and $\partial U/\partial y$ can be determined from the fringe slopes. The fringe gradients in the different plies can be measured effectively. The shear strain distribution along line A is plotted in Fig. 4d, using data from this pattern and the corresponding V field. The different strain levels in successive plies are caused by their different stiffnesses in shear. The high peaks occur at the resin-rich zones between plies, where high shear compliance leads to localized high shear strains.

3.4 Carrier Patterns in Both Directions

Figure 5 illustrates an interlaminar compression test of a thick composite. The material was graphite/epoxy, with a [90/90/0]n stacking sequence, i.e., two plies with fibers in the x direction followed by one ply with fibers in the z direction, repeated many times. The specimen was 15 mm tall with 13x13 mm cross-section.

The V displacement field is shown in Fig. 5b for the portion in the dashed box (Fig. 5a). The strains could be determined easily in the 90 deg plies, by $\varepsilon = G_y/f$. In the 0 deg plies, however, the fringes are too few to determine their gradient. The pattern was transformed to that of Fig. 5c by adding carrier patterns of both extension and rotation. First, a carrier pattern of extension was applied; it was equal in magnitude and opposite in sign to the gradient in 90 deg plies, such that the resulting gradient in 90 deg plies became approximately zero. Then a carrier pattern of rotation was applied to produce Fig. 5c. Near point A, the fringes in 90 deg plies are vertical. This indicates no additional y direction gradient. In 0 deg plies, the fringes have an angle ϕ_1 and in resin-rich zones between plies they have an angle ϕ_2. The corresponding strains ε_y are calculated by

$$\varepsilon_y = G_x \tan\phi + \varepsilon_{90}$$

where ε_{90} is the normal strain in the 90 deg plies, i.e., the strain that was subtracted off by the carrier pattern of extension. The result is plotted in Fig. 5d, which shows essentially uniform compressive strains through the thickness of each ply and strong strain peaks in the resin-rich zones between plies. Clearly, this detail would be extremely difficult to extract from the load-induced pattern without the use of carrier patterns.

4.0 CONCLUSIONS

By using carrier patterns, the detailed information extracted from moire patterns can be vastly increased and the procedure for extracting data can be easier and more accurate. The carrier patterns are easily introduced and controlled by adjustments of the moire interferometry optical system. Considering its simplicity, the benefits seem magical!

5.0 ACKNOWLEDGEMENTS

This work was sponsored by The National Center for Composite Materials Research, Urbana, Illinois, and it was encouraged by Dr. Alan Kushner of the Office of Naval Research. This generous support is gratefully acknowledged.

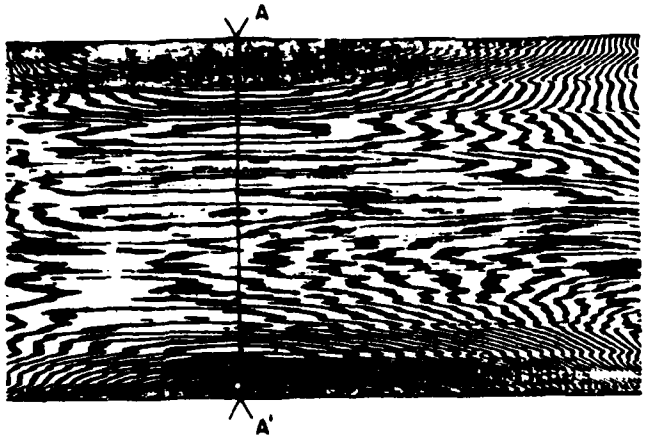

b. Load-induced fringe pattern of the U field for portion of specimen in dashed box

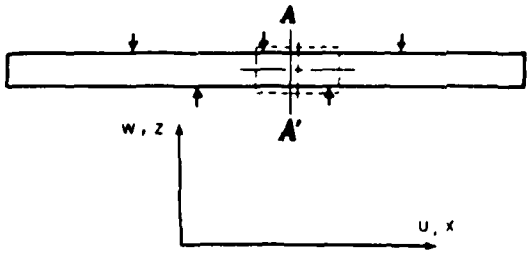

a. Specimen and loading

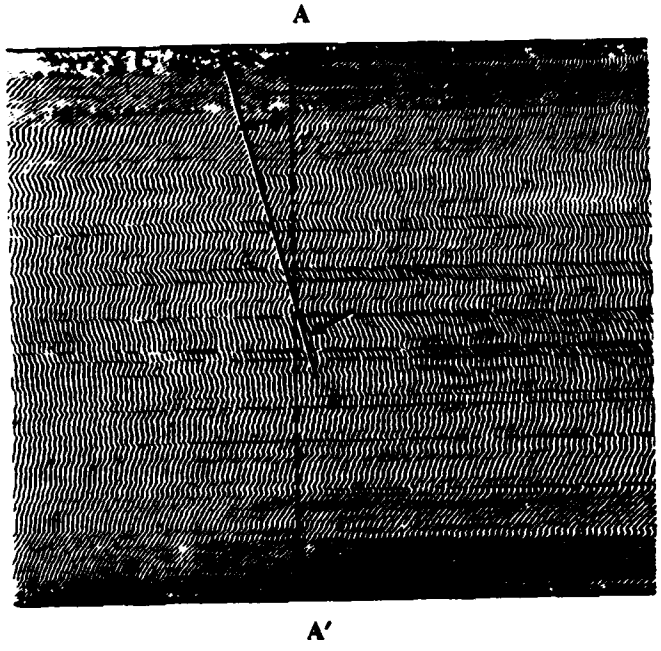

c. Load-induced fringes with carrier pattern of extention

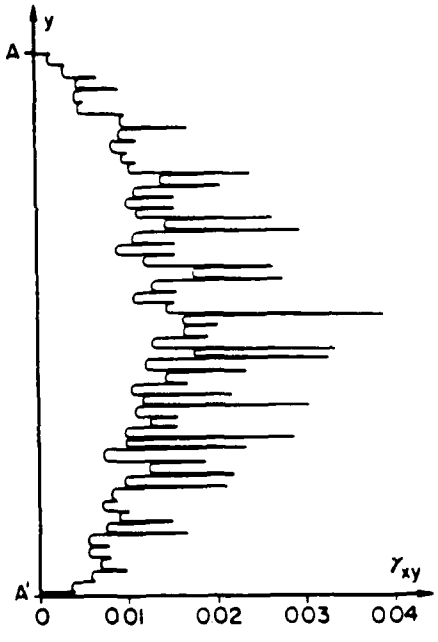

d. Shear strain distribution along the line A-A'

Fig. 4. Five-point Bending Beam Test of [+45/0/-45/90]6s Graphite-PEEK Composite Specimen.

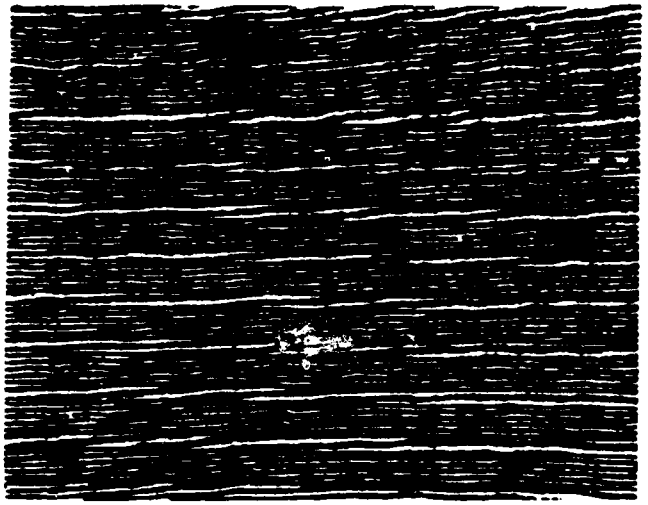

b. Load-induced fringe pattern of the V field for portion of specimen in dashed box

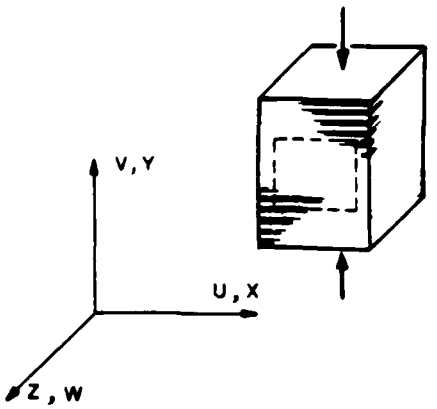

a. Specimen and loading

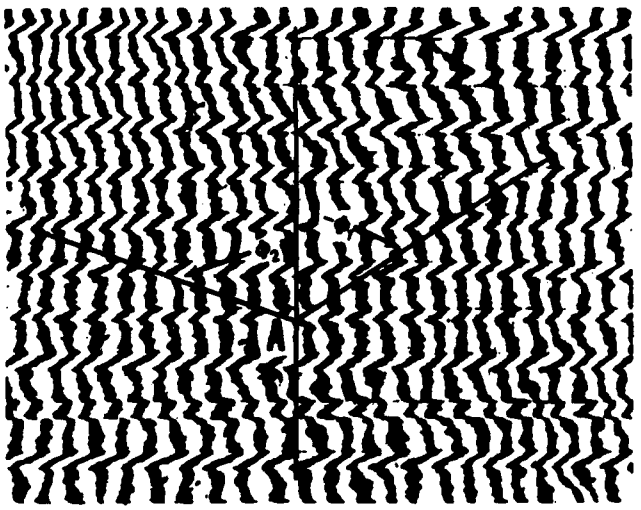

c. Load-induced fringes with carrier patterns of extension and rotation

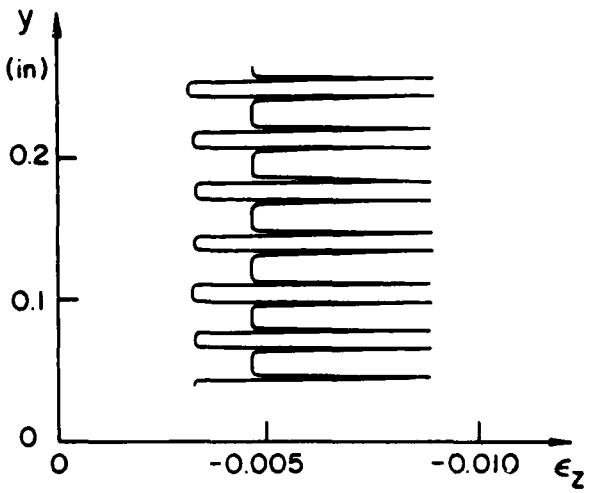

d. Compressive strain distribution along vertical line. Note this is representative since material properties and strains vary throughout the specimen

Fig. 5. Interlaminar Compression Test of [90/90/0]n Graphite/Epoxy Composite Specimen.

6.0 REFERENCES

1. D. Post, "Moire Interferometry," Chap. 7, Handbook of Experimental Mechanics, A. S. Kobayashi, Editor, Prentice-Hall, Englewood Cliffs, NJ (1987).

2. V. J. Parks, "Geometric Moire," Chap. 6, Handbook of Experimental Mechanics, A. S. Kobayashi, Editor, Prentice-Hall, Englewood Cliffs, NJ (1987).

3. Fu-Pen Chiang, "Moire Method of Strain Analysis,", Chap. 6, Manual on Experimental Stress Analysis, A. S. Kobayashi, Editor, Society for Experimental Stress Analysis, Bethel, CT (1978).

4. M. L. Basehore and D. Post, "Displacement Fields (U,W) Obtained Simultaneously by Moire Interferometry," Applied Optics, 21(14), pp. 2558-2562 (July 15, 1982).

5. R. Czarnek, D. Post, Y. Guo, "Nonuniformaties in Composite Panels by Moire Interferometry," Proceedings of the 1986 SEM Spring Conference on Experimental Mechanics, SEM, Bethel, CT (June 1986).

6. D. Post, R. Czarnek and D. Joh, "Shear Strain in a Graphite-PEEK Beam by Moire Interferometry with Carrier Fringes," Experimental Mechanics, Vol. 27, 1987 (to be published).

END

DATE

FILMED

FEB.

1988